ENHANCED KNOWLEDGE IN SCIENCES AND TECHNOLOGY
e-ISSN: 2773-6385

EKST

Vol. 4 No. 2 (2024) 635-648
https://publisher.uthm.edu.my/periodicals/index.php/ekst

DNA Barcoding of Selected Zombie-Ant Fungi in Hutan Simpan Labis, Johor

Kenneth Yohansen Kendawang[1], Jeremiah Sia Yiao Rong[1], Yap Jing Wei[1*,]

[1] *Department of Technology and Natural Resources, Faculty of Applied Sciences and Technology, Universiti Tun Hussein Onn Malaysia (Pagoh Campus), Pagoh Higher Education Hub, Muar, Johor MALAYSIA*

*Corresponding Author : jwyap@uthm.edu.my
DOI: https://doi.org/10.30880/ekst.2024.04.02.069

Article Info

Received: 27 December 2023
Accepted: 13 January 2024
Available online: 12 December 2024

Keywords

Ophiocordyceps, fungi, entomopathogenic fungi, DNA barcoding, host, insect

Abstract

Ophiocordyceps is a genus of entomopathogenic fungi that has garnered increasing attention in recent years due to its diverse ecological roles and promising biomedical applications. However, the *Ophiocordyceps* species diversity is still unknown especially in Peninsular Malaysia. This study was conducted to identify the species of ant-infecting *Ophiocordyceps* present in Hutan Simpan Labis (west Endau-Rompin) using DNA barcoding with SSU and *tef*. In addition, it also aims to document the sexual and asexual morphology of the selected *Ophiocordyceps*. The preliminary SSU and *tef* DNA results and morphology suggests that the sample in Hutan Simpan Labis is most likely *O.* cf. *unilateralis.* This study has generated the first SSU and *tef* DNA sequences and reported the fungal morphology for the *Ophiocordyceps* in Hutan Simpan Labis.

1. Introduction

Zombie ant fungi (*Ophiocordyceps*), are a form of entomopathogenic fungi, that infect ants and modify their behavior. When an ant becomes infected, the fungus seizes control of its motion and compels it to ascend to a higher elevation and thus, attach itself to a leaf or stem. Following the ants' demise, the fungi emerge from its body and spreads to other ants by dispersing its spores. Although *Ophiocordyceps* are best known as parasites of ants, their known host range is in fact much wider and extends to various insect orders, including Hemiptera, Hymenoptera, Coleoptera, Lepidoptera, Megaloptera, Odonata, Orthoptera, Blattaria, and Diptera (Araújo & Hughes, 2019). *Ophiocordyceps* are known from various types of tropical to temperate forests throughout the world and have been reported from Asia, North and South America, Africa and Australia. Although *Ophiocordyceps* are known to occur in Peninsular Malaysia, the precise distribution and species composition of *Ophiocordyceps* in Peninsular Malaysia is still not known and likely contains undocumented species.

DNA barcoding is really a vital component in order to gain accurate species identification, especially in cases where the morphological identification alone may be challenging or difficult to observe. By establishing this DNA barcodes, this study will provide a robust and reliable tool for future identification and classification of entomopathogenic fungi in Peninsular Malaysia.

Hutan Simpan Labis is a relatively unexplored forest area in west of Endau-Rompin National Park, Johor. This study aims to identify the *Ophiocordyceps* species using DNA barcoding and document the morphology of the fungi.

2. Material and methods

2.1 Sampling

Sampling were undertaken in the area of Hutan Simpan Labis such as Taka Melor, Hutan Lipur and Sungai Bantang. The sampling protocol consisted of intense inspection of the leaf litter, shrub leaves and tree trunks estimated from 1 m to 2 m high. The leaves was excavated in search for specimens attached to host insects, especially near the street or river [14]. The handling and preservation of the samples was placed inside sterile plastic containers to maintain their integrity during transportation to the microbiology laboratory at UTHM.

2.2 Morphological Identification

Morphological identification for macro-morphological characterization sample was identified using a stereoscopic microscope (OLYMPUS SZX16). The characters investigated were: host location for instance, spine, trunk, moss, base of trunk, and soil. For sexual structures, key characteristics such as stroma colour, ascoma (fruiting body) morphology, perithecia (sac-like structures), asci (spore-containing sacs), and ascospores were examined [24][28]. Additionally, asexual structures like phialides (spore-producing cells) and conidia (asexual spores) were observed [28]. To facilitate accurate identification, samples was prepared for microscopic analysis by cutting open the structures and creating thin sections using a blade [24]. A compound microscope (OLYMPUS CX22LED) was used for further examination and documentation of the morphological characteristics of which fungi it is.

A mixture comprising 24g potato dextrose grains and 15g agar powder in distilled water was autoclaved at 121 ℃ for 15 minutes. Following autoclaving, 2ml of 0.05g/ml streptomycin sulphate was added, and the mixture was poured onto petri plates to solidify. Even distribution of the sample was conducted inside biosafety cabinet and applied across the surface of the agar, allowing the mycelium to grow and colonize the medium. The plates were sealed and incubated under specific temperature (27℃) and humidity conditions suitable for the growth of fungi [24]. Observation of the growth patterns were conducted to evaluate the morphological characteristics and documentation was written for any changes or developments. Regular checks were also performed to assess the health and viability of the cultures.

2.3 DNA Extraction

All the species proposed in this study were collected in their natural habitat. The DNA templates were obtained directly from the specimens with the following protocol from DNA extraction fungal/bacteria kit (ZYMO RESEARCH) : 25 mg sample was cleaned thoroughly and submerged t distilled water three times. The sample was added to a ZR BashingBead™ Lysis Tube (0.1 mm & 0.5mm) followed by 750 µl BashingBead™ Buffer was added to the tube to the tube[2]. A bead beater was secured then processed in the machine at speed 3.10 for 5 minutes (round 1) then speed 2.10 for 5 minutes. 3. ZR BashingBead ™ Lysis Tube (0.1 & 0.5 mm) was centrifuged in a microcentrifuge at 10,000 x g for 1 minute. 400 µl supernatant to a Zymo-Spin™ III-F Filter was transferred in a collection tube and centrifuge at 8,000 x g for 1 minute. 1,200 µl of Genomic Lysis Buffer to the filtrate in the previous collection tube. 800 µl of the mixture from collection tube was to a Zymo-Spin™ IICR Column in a new collection tube and centrifuge at 10,000 x g for 1 minute. Flow through from the collection tube was discarded then repeated once more with the remainder mixture. 200 µl DNA Pre-Wash Buffer was added to the Zymo-Spin ™ IICR Column in a new collection tube and centrifuge at 10,000 x g for 1 minute. 500 µl g-DNA Wash Buffer then was added to the Zymo-Spin ™ IICR Column and centrifuge at 10,000 x g for 1 minute. Zymo-Spin™ IICR Column was transferred to a clean 1.5 ml microcentrifuge tube and 50 µl (35 µl minimum) DNA Elution Buffer was added directly to the column matrix followed by conducted microcentrifuge at 10,000 x g for 30 seconds to elute the DNA.

2.4 Polymerase Chain Reaction (PCR)

Three region were used in the analyses, i.e. small subunit nuclear ribosomal DNA (SSU), large subunit nuclear ribosomal DNA (LSU), translation elongation factor 1-α (*tef*). The primers used were, SSU: NS1 (GTAGTCATATGCTTGTCTC) and NS4 (CTTCCGTCAATTCCTTTAAG); LSU: LR0R (5'-ACCCGCTGAACTTAAGC-3') and LR5 (5'-TCCTGAGGGAAACTTCG-3'); *tef*: 983F (50-GCYCCYGGHCAYCGTGAYTTYAT-3'). Go Taq™ Green Master Mixes was used to amplify PCR reaction[29][30].

Each 25 µL-PCR reaction contained of 5 µL 5x or colorless GoTaq flexi Buffer, 1.5 µl $MgCl_2$ (solution 25mm) , 0.5 µl PCR nucleotide mix (10mM each), 2 µL upstream and downstream primer (10µM each, 0.126 µL GoTaq DNA polymerase (5µ/Hl), 10µL of DNA template and 3.8.74 µL of sterile distilled water

The PCR reactions were placed in a thermocycler under the following conditions: for SSU and LSU (1) 2 min at 94 °C, (2) 4 cycles of denaturation at 94 °C for 30 s, annealing at 55 °C for 30 s, and extension at 72 °C for 2 min, followed by (3) 35 cycles of denaturation at 94 °C for 30 s, annealing at 50.5 °C for 1 min, and extension at 72 °C for 2 min and (4) 3 min at 72 °C. For *tef* (1) 2 min at 94 °C, (2) 10 cycles of denaturation at 94 °C for 30 s, annealing

at 64 °C for 1 min, and extension at 72 °C for 1 min, followed by (3) 35 cycles of denaturation at 94 °C for 30 s, annealing at 54 °C for 1 min, and extension at 72 °C for 1 min and (4) 3 min at 72 °C.

Agarose gels were prepared by dissolving 6 g of agarose powder in 40 mL of 1xTAE in a beaker. The mixture was microwaved for one minute until the agarose was fully dissolved. Subsequently, the agarose solution was allowed to cool down to approximately 50 °C before adding 3 µl of DNA stain to the gel. The prepared gel was then poured into a gel box with a suitable gel comb, and it was left to harden for 30 minutes.

All PCR products were evaluated by agarose gel electrophoresis against a DNA ladder. All samples that produced a clear band within the expected size range were sent to the Genetics Laboratory, Forest Research Institute Malaysia for sequencing.

2.5 Data Analysis

Data analysis was conducted using Geneious v9.1.8. Raw data, consisting of electropherograms, were edited, trimmed, assembled into contigs and used to generate consensus sequences. Identification of sequences was achieved using GenBank Basic Local Alignment Search Tool (BLAST) search using default settings. DNA sequences were aligned into a matrix with outgroup fungal sequences from GenBank (Table 2.1). Phylogenetic analysis was carried out using the neighbour-joining (NJ) method using the Geneious Tree Builder tool using the following settings: *Purpereocillium sp*. and *Purpureocillium lilanicum* were included as outgroup taxa as well as 19 ingroups of sequences , serving as the root for the phylogenetic tree.

Table 2.1 *Incorporated species for phylogenetic analyses of Ophiocordyceps spp. using SSU and tef gene.*

Species Identity	Sample size	Individual number	Genbank accession number
Ophiocordyceps pseudorhozoiddea	1	BCC 86431	MK284262.1
Ophiocordyceps asiatica	1	BCC 30516	MK284263.1
Ophiocordyceps bidoupiensis	1	YFCC8793	OK556894.1
	1	YHH 20036	OK556893.1
Ophiocordyceps khokpasiensis	1	BCC 48071	MK284269.1
Ophiocordyceps mosingtoensis	1	BCC 36921	MK284272.1
Ophiocordyceps sp.	4	YFCC 5079243	OQ622099.1
		YFCC 5079245	OQ622102.1
		NHJ 01164	JN940996
		*MS2	
		*S28	
Ophiocordyceps clavata	1	NRBC 106961	JN941727.1
Ophiocordyceps irangiensis	1	NRBC 101400	JN941715.2
Ophiocordyceps appendiculata	1	NRBC 106959	JN941729.1
Ophiocordyceps pseudolloydii	2	MFLU:22-0266	OQ186385
		XS 65	ON890866
Ophiocordyceps cf. unilateralis	1	MY 5151	GU797110
Ophiocordyceps unilateralis	1	SERI 2	KX713627
Ophiocordyceps rubiginosiperithea	1	NRBC 106966	JN941704.1

Ophiocordyceps spechocephala	1	NRBC 101416	JN941698
Ophiocordyceps stylophora	1	NRBC 100947	JN941694.1
Ophiocordyceps halabalaensis	1	MY5 151	KM655826
Purpureocillium sp.	1	A 15693	MF787282.1
Purpureocillium lilanicum	1	Arsef 2181	AF339583.1

Notes: *indicates sequences generated in this study. The ones without the bullet symbol were corresponding sequences obtained from the GenBank, NCBI,US National Library of Medicine.

3. Result and Discussion

3.1 Morphological Characteristics

Fig. 3.1 shows an example of the mature sexual fruiting body emerging from the ant host. The fruiting body is composed of phialides, flask-shaped cells, give rise to conidia, which serve as asexual spores facilitating the infection of new hosts. The collective arrangement of phialides forms conidiophores, contributing to the development of a stalked structure emerging from the host exoskeleton, enabling the dispersal of conidia for further host infection[21][28]. The sexual structures initiate with the formation of ascomata, or ascomata-like structures, known as ascomata in fungal taxonomy. Within these structures, perithecia (Fig. 3.2) develop, flask-shaped structures containing asci. Asci shown in Fig. 3.2 house ascospores, the sexual spores released into the environment to promote genetic recombination and enhance the adaptability of the fungus[21].

The identity of the host ant is unclear due to fungal growth which obscured the diagnostic characters. However, the overall morphology resembles that of species from the *O. unilateralis* complex. Further work needs to be done to determine the species of host.

(a) **(b)**

Fig. 3.1 *(a) Fruiting body emerging from infected and host; (b) Close up of fruiting body*

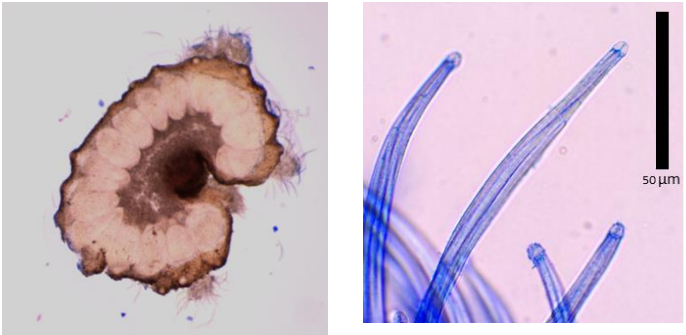

(a) **(b)**

Fig. 3.2 *(a) Perithecia; (b) Asci*

Enhanced Knowledge in Sciences and Technology Vol. 4 No. 2 (2024) p. 635-648

3.2 Ecological Identification

Identification of the samples collected in the west Endau Rompin area (Hutan Lipur, Taka Melor, and Sungai Bantang. The pie charts in Fig. 3.3 summarizes the location and micro-environments of the *Ophiocordyceps* samples collected in this study.

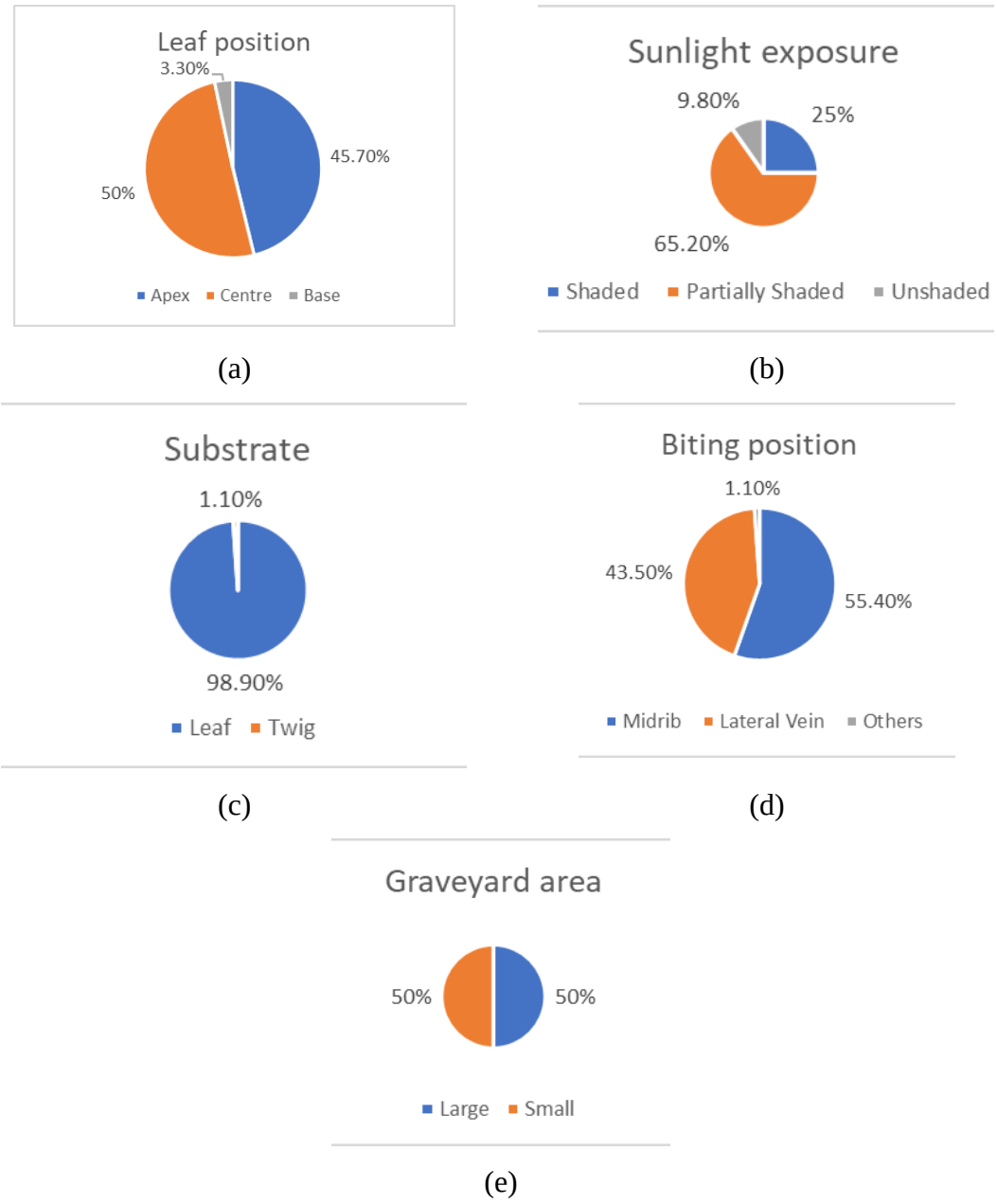

Fig 3.3 *(a) Leaf position host located, (b) Sunlight exposure to the sample, (c) Sample substrate (twig/leaf), (d)Sample biting position on leaf, (e) Amount of graveyard area found*

A total of 92 individual samples were collected in this study. The majority of infected hosts were found at the apex (45.7%), followed by the center (50%) and only a small percentage at the base (3.3%). This distribution suggests a preference of the pathogen for specific leaf positions. The higher prevalence at the apex and center could be attributed to factors such as increased vulnerability or better conditions for pathogen development.

The prevalence of infected hosts in different sunlight exposures varied significantly. The majority were found in partially shaded areas (65.2%), followed by shaded areas (25%) and unshaded areas (9.8%). This highlights a

potential correlation between sunlight exposure and pathogen prevalence, indicating that the pathogen may thrive better under certain light conditions.

Almost all infected hosts were found on leaves (98.9%), with only a negligible percentage on twigs. This emphasizes a strong association between the pathogen and leaf substrate. The specific conditions provided by leaves may favor the pathogen's life cycle or make it more conducive for infection.

The distribution of infected hosts based on biting position reveals a relatively equal prevalence on midribs (55.4%) and lateral veins (43.5%). This suggests that the pathogen does not show a clear preference for either midribs or lateral veins which suggests a degree of phenotypic plasticity in this feature.

The equal distribution of infected hosts in large and small graveyards (50% each) might indicate that graveyard size does not significantly influence the prevalence of the pathogen. Other factors, such as micro-climatic conditions or host plant characteristics, may play a more substantial role in determining the pathogen's prevalence. The large graveyard area is an area where the infecting process has occurred over a long period of time since many infected specimens are found in the area, while small graveyard area may indicate areas where infection is still new and has not yet spread the spores to the insects below causing only a few the number of samples in the tree is small. This understanding helps to identify whether the sample has released its spore to other insects or not in a short time or not.

3.3 DNA Sample Collection

The DNA was successfully extracted from multiple samples using of DNA Extraction Fungal/Bacteria Kit by Zymo Research. Table 3.1 show the list of DNA sample collected through extraction.

Table 3.1 *DNA sample collection for extraction*

Sample	Source	Location
MS1	Fungal stalk	Taka Melur
MS2	Fungal stalk	Taka Melur
S28	Fungal stalk	Sungai Bantang

3.4 PCR

Above 1,000 base pair (bp) gene fragments were successfully amplified from MS1, MS2 and S28. All three samples also went through repeated PCR to obtain more segment of DNA. Figure 3.4 show high quantity of PCR product and sufficient for DNA sequencing for MS1 and S28 sample. For LSU region in figure 3.5 was also conducted repeated PCR as the band does not show high concentration and as probably the DNA concentration of DNA sample is low for all the sample for the region.

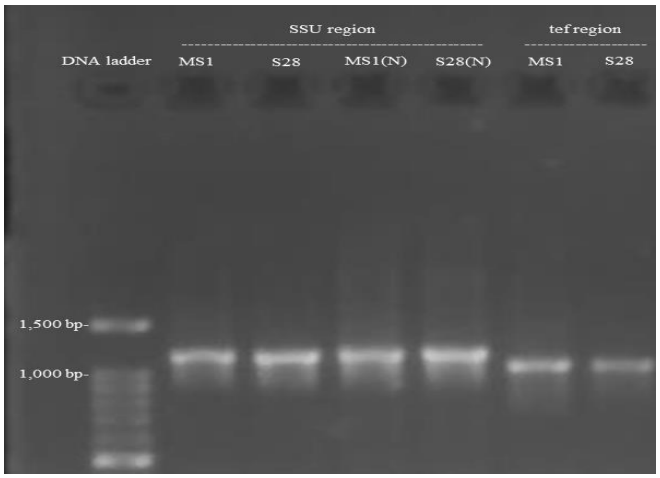

Fig. 3.4 *PCR result of ribosomal RNA of SSU and tef protein using BIO-5130 ExactMark 100bp DNA Ladder (100-1,500bp)*

Notes: N-*nested PCR*

Enhanced Knowledge in Sciences and Technology Vol. 4 No. 2 (2024) p. 635-648

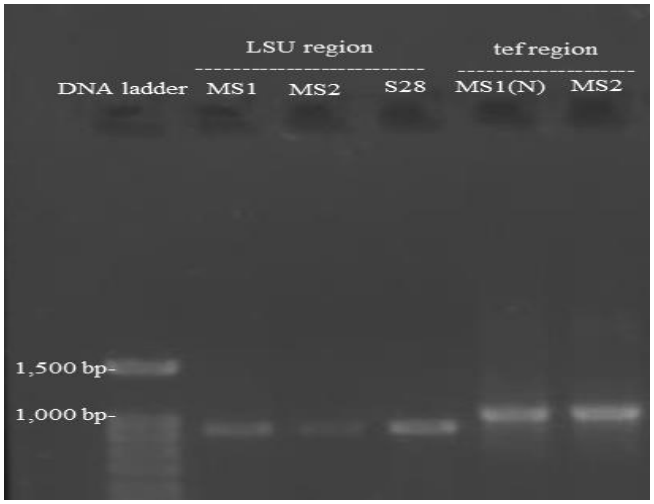

Fig. 3.5 *PCR results of coding gene sequences of all three sample for LSU and tef region using BIO-5130 ExactMark 100bp DNA Ladder (100-1,500bp)*

Notes: N-*nested PCR*

3.5 Sequence Analysis

Of the nine samples sequenced, only two produced both *tef* and SSU sequences that could be used for analysis, namely MS2 for *tef* while S28 was only for SSU. Others did not succeed even though there were sequences because the number of base pairs was insufficient and could not be assembled. The DNA sequences for MS2 (Fig. 3.6) and S28 (Fig. 3.7) was visualized and assembled using Geneious Prime (Biomatters Ltd.) software. This was done to observe the high peak of the DNA sequences that are rarely overlapping with each other.Meanwhile, MS1 was not able to be assembled due to the mishap and does does not have desired DNA sequences.

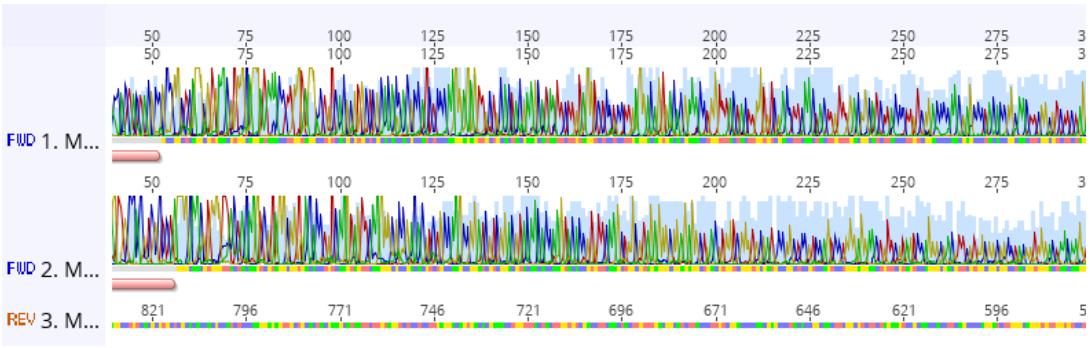

Fig. 3.6 *Part of forward and reverse DNA sequences of MS2 visualized using Geneious Prime (Biomatters Ltd.)*

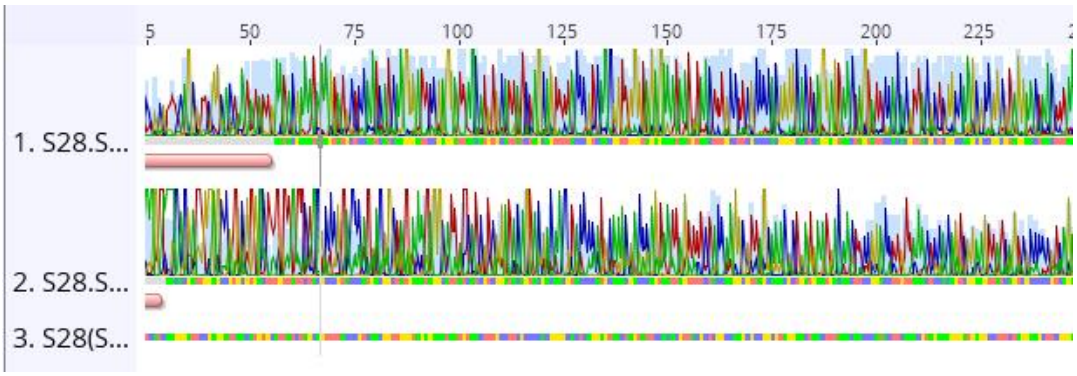

Fig. 3.7 *Part of forward and reverse DNA sequences of S28 visualized using Geneious Prime (Biomatters Ltd.)*

3.6 Nucleotide BLAST

The identity of the sequences was checked using an online Basic Local Alignment Search Tool program for nucleotide (Nucleotide BLAST) to align and match each gene sequence from this study with available *Ophiocordyceps spp.* gene sequences in the GenBank National Center for Biotechnology Information (NCBI), U.S. National Library of Medicine. Fig. 3.8 shows the nucleotide BLAST results of DNA sequences of MS2 and Fig. 3.9 for nucleotide BLAST result for S28

Description	Scientific Name	Max Score	Total Score	Query Cover	E value	Per. Ident	Acc. Len	Accession
Ophiocordyceps sp. DXT-2022f strain YFCC 8817 translation elongation factor 1 alpha (tef) gene, partial cds	Ophiocordyceps ...	1435	1435	100%	0.0	96.44%	930	ON567756.1
Ophiocordyceps sp. DXT-2022f strain YFCC 8816 translation elongation factor 1 alpha (tef) gene, partial cds	Ophiocordyceps ...	1435	1435	100%	0.0	96.44%	930	ON567755.1
Ophiocordyceps sp. DXT-2022f strain YFCC 8814 translation elongation factor 1 alpha (tef) gene, partial cds	Ophiocordyceps ...	1435	1435	100%	0.0	96.44%	930	ON567754.1
Ophiocordyceps sp. DXT-2022f strain YFCC 8815 translation elongation factor 1 alpha (tef) gene, partial cds	Ophiocordyceps ...	1435	1435	100%	0.0	96.44%	930	ON567753.1
Ophiocordyceps sp. DXT-2022b strain YHH 20191 translation elongation factor 1 alpha (tef) gene, partial cds	Ophiocordyceps ...	1408	1408	100%	0.0	95.86%	927	ON567748.1
Ophiocordyceps sp. strain YHH 20037 translation elongation factor 1-alpha (TEF) gene, partial cds	Ophiocordyceps ...	1375	1375	100%	0.0	95.17%	930	OL322693.1
Ophiocordyceps sp. strain YFCC 8796 translation elongation factor 1-alpha (TEF) gene, partial cds	Ophiocordyceps ...	1375	1375	100%	0.0	95.17%	930	OL322692.1
Ophiocordyceps sp. strain YHH 20038 translation elongation factor 1-alpha (TEF) gene, partial cds	Ophiocordyceps ...	1369	1369	100%	0.0	95.06%	930	OL322694.1
Ophiocordyceps sp. strain YFCC 8795 translation elongation factor 1-alpha (TEF) gene, partial cds	Ophiocordyceps ...	1369	1369	100%	0.0	95.06%	930	OL322688.1
Ophiocordyceps sp. DXT-2022a strain YFCC 9017 translation elongation factor 1 alpha (tef) gene, partial cds	Ophiocordyceps ...	1363	1363	100%	0.0	94.94%	930	ON567759.1
Ophiocordyceps unilateralis strain KT3308 translation elongation factor 1 alpha (tef) gene, partial cds	Ophiocordyceps ...	1363	1363	100%	0.0	94.94%	932	GU797112.1
Ophiocordyceps unilateralis strain KT3307 translation elongation factor 1 alpha (tef) gene, partial cds	Ophiocordyceps ...	1363	1363	100%	0.0	94.94%	918	GU797111.1

Fig. 3.8 *Nucleotide Basic Local Alignment Search Tool (Nucleotide BLAST) results of DNA sequences of MS2.*

Description	Scientific Name	Max Score	Total Score	Query Cover	E value	Per. Ident	Acc. Len	Accession
Ophiocordyceps camponoti-leonardi (nom. inval.) voucher MFLU:22-0269 small subunit ribosomal RNA gene, pa...	Ophiocordyceps ...	1792	1792	100%	0.0	99.80%	1023	OQ127319.1
Ophiocordyceps sp. DXT-2022e strain YHH 20168 small subunit ribosomal RNA gene, partial sequence	Ophiocordyceps ...	1786	1786	99%	0.0	99.79%	1008	ON555849.1
Cordyceps unilateralis strain OSC 128574 small subunit ribosomal RNA gene, partial sequence	Ophiocordyceps ...	1775	1775	100%	0.0	99.49%	1018	DQ522554.1
Ophiocordyceps ootakii strain J14 small subunit ribosomal RNA gene, partial sequence	Ophiocordyceps ...	1773	1773	100%	0.0	99.49%	1020	KX713651.1
Ophiocordyceps sp. DXT-2022c strain YFCC 9048 small subunit ribosomal RNA gene, partial sequence	Ophiocordyceps ...	1773	1773	100%	0.0	99.49%	1008	ON555847.1
Ophiocordyceps sp. DXT-2022c strain YHH 20163 small subunit ribosomal RNA gene, partial sequence	Ophiocordyceps ...	1773	1773	100%	0.0	99.49%	1003	ON555845.1
Ophiocordyceps sp. DXT-2022c strain YHH 20162 small subunit ribosomal RNA gene, partial sequence	Ophiocordyceps ...	1773	1773	100%	0.0	99.49%	1027	ON555844.1
Ophiocordyceps sp. DXT-2022c strain YFCC 9012 small subunit ribosomal RNA gene, partial sequence	Ophiocordyceps ...	1773	1773	100%	0.0	99.49%	1030	ON555843.1
Ophiocordyceps satoi strain YFCC 8810 small subunit ribosomal RNA gene, partial sequence	Ophiocordyceps ...	1773	1773	100%	0.0	99.49%	1008	OP782342.1
Ophiocordyceps satoi strain YFCC 8809 small subunit ribosomal RNA gene, partial sequence	Ophiocordyceps ...	1773	1773	100%	0.0	99.49%	1008	OP782341.1
Ophiocordyceps satoi strain YFCC 8807 small subunit ribosomal RNA gene, partial sequence	Ophiocordyceps ...	1773	1773	100%	0.0	99.49%	1008	OP782340.1
Ophiocordyceps sp. strain YFCC 8796 small subunit ribosomal RNA gene, partial sequence	Ophiocordyceps ...	1772	1772	100%	0.0	99.39%	1011	OL310722.1
Ophiocordyceps naomipierceae strain DAWKSANT small subunit ribosomal RNA gene, partial sequence	Ophiocordyceps ...	1768	1768	100%	0.0	99.39%	1034	KX713664.1
Ophiocordyceps sp. DXT-2022c strain YFCC 9013 small subunit ribosomal RNA gene, partial sequence	Ophiocordyceps ...	1768	1768	99%	0.0	99.49%	1007	ON555848.1

Fig. 3.9 *Nucleotide Basic Local Alignment Search Tool (Nucleotide BLAST) results of DNA sequences of MS2.*

The Nucleotide BLAST results showed that the MS2 sample belongs to the *Ophiocordyceps* genus. Further, MS2 most closely matches as *Ophiocordyceps sp.* DXT-2022 with 96.44% of identity when aligned against the corresponding sequences including the first match with GenBank accession number of ON567756.1, while S28 sample were identified as *Ophiocordyceps camponiti-leonardi* with 99.80% of identity when aligned against the corresponding sequences including the first match with GenBank accession number of OQ127319.1

The score of query cover for the Nucleotide BLAST of the *Ophiocordyceps sp.* was 100% and the expected value (E value) was zero showing the most significant score and alignment with the corresponding sequences. Both max score and total score for *Ophiocordyceps sp.* were 1435. On the other hand, the scores of query cover and the expected value (E value) were zero showing the most significant score and alignment with the corresponding sequences. Both max score and total score for *Ophiocordyceps camponiti-leonardi* were 1792. Thus, the findings suggested that the sample collected from West Endau-Rompin is came from *Ophiocordyceps* genus.

3.7 Translated Elongation Factor (*tef*) Gene

The evolutionary history was inferred using the Neighbor-Joining method [26]. The optimal tree with the sum of branch length = 0.7197 is shown. The percentage of replicate trees in which the associated taxa clustered together in the bootstrap test (1000 replicates) are shown next to the branches [25]. The tree (Fig. 3.8) is drawn to scale, with branch lengths in the same units as those of the evolutionary distances used to infer the phylogenetic tree. The evolutionary distances were computed using the Kimura 2-parameter method [27] and are in the units of the number of base substitutions per site. The analysis involved 11 which was ten of it from *Ophiocordycyceps spp.*

and one from *Purpureocilium sp.*. The analysis was conducted by using Geneious Prime. Figure 3.10 shows the *tef* NJ tree. In this tree, MS2 was found to resolve with *O.* cf. *unilateralis* with 100% support which suggests that MS2 is most likely *O*. cf. *unilateralis* from Thailand.

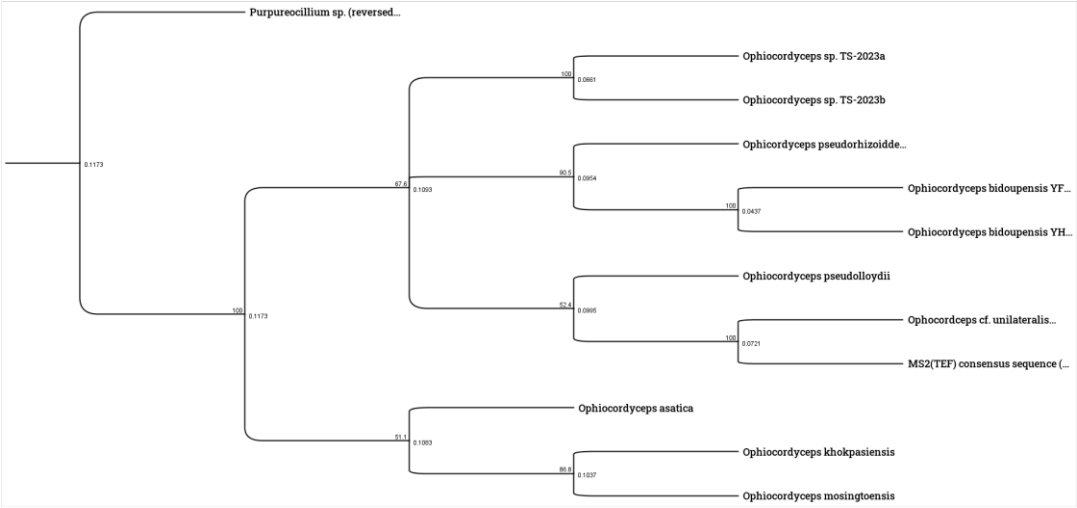

Fig. 3.10 *The Neighbor-Joining (NJ) phylogenetic tree based on translation elongated factor (tef) sequences for MS2. The numbers at the branches stand for bootstrap value (%) 1000 replications.*

3.8 Small Subunit Ribosomal (SSU) Gene

The evolutionary history was inferred using the Neighbor-Joining method[26]. The optimal tree with the sum of branch length = 4.0134 is shown. The percentage of replicate trees in which the associated taxa clustered together in the bootstrap test (1000 replicates) are shown next to the branches [25]. The tree (Fig. 3.11) is drawn to scale, with branch lengths in the same units as those of the evolutionary distances used to infer the phylogenetic tree. The evolutionary distances were computed using the Kimura 2-parameter method and are in the units of the number of base substitutions per site [27]. The analysis involved 11 which was ten of it from *Ophiocordyceps spp.* and one from *Purpureocilium sp.* The tree shows that S28 resolving into a clade with *Ophiocordyceps halabalaensis* with 96% bootstrap value. This suggests that S28 is closely related to *Ophiocordyceps halabaensis* from Thailand. This species also show that they are pathogenic against *Camponiti* genus such as *Camponiti gigas.*

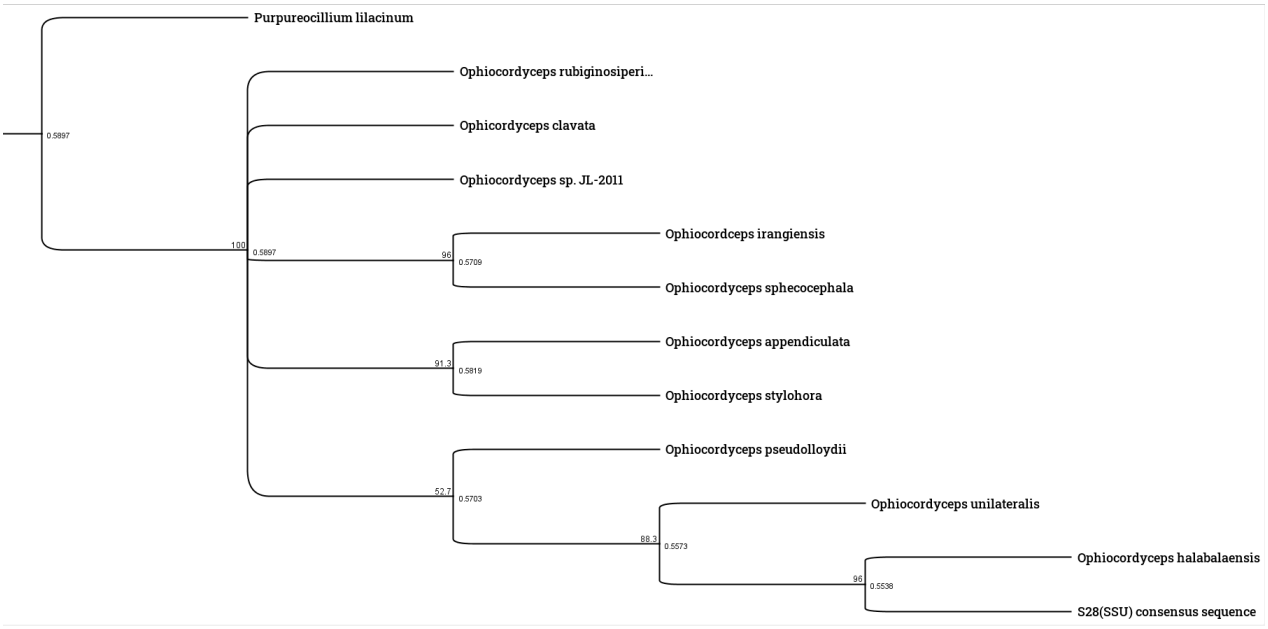

Fig. 3.11 *The Neighbor-Joining (NJ) phylogenetic tree based on small subunit(SSU) sequences for S28. The numbers at the branches stand for bootstrap value (%) 1000 replications.*

4. Conclusion

In conclusion, this study has successfully produced the first *tef* and SSU DNA barcodes sequences and documented the morphology for *Ophiocordyceps* from Hutan Simpan Labis. In addition, the preliminary DNA sequences and morphology results suggest that it is most closely related to *O. halabalaensis* and *O. cf. unilateralis* from Thailand. However, further work needs to be done to verify the exact species identity as comprehensive analysis was not possible due to time and cost limitations. Future work should include the sequencing of additional DNA barcode sequences, high-throughput sequencing and identification of the host ant are needed. To our knowledge, this study represents the first ever report on the DNA barcodes for *Ophiocordyceps* from Hutan Simpan Labis and Peninsular Malaysia.

Acknowledgement

I would like to express my sincere gratitude to my colleagues Umirul Akmalissa and Shalini and for their continuous support and collaborative efforts during conducting this research. Finally, this study was supported by funds from the Fundamental Research Grant Scheme (FRGS/1/2023/WAB11/UTHM/02/1) by the Ministry of Higher Education. I also would like to express their sincere gratitude to the Johor Forestry Department for their invaluable support and cooperation throughout the research as to give us permission to enter Hutan Simpan Labis and allow us to collect sample for the sake of this study.

Conflict of Interest

Authors declare that there is no conflict of interests regarding the publication of the paper.

Author Contribution

The authors confirm contribution to the paper as follows: ***study conception and design, data collection, methodology, analysis and interpretation of results:*** *Kenneth Yohansen Kendawang, Jeremiah Sia Yiao Rong and Yap Jing Wei. All authors reviewed the results and approved the final version of the manuscript.*

Appendix A: Table Distribution of Collected Sample

Sample	Location	Death position	Leaf position	Distribution
1	Taka Melor	Midrib	Apex	
2	Taka Melor	Midrib	Center	
3	Taka Melor	Midrib	Apex	
4	Taka Melor	Midrib	Apex	Large Graveyard area 1
5	Taka Melor	Midrib	Apex	Large Graveyard area 1
6	Taka Melor	Lateral vein	Center	Large Graveyard area 1
7	Taka Melor	Lateral vein	Apex	Large Graveyard area 1
8	Taka Melor	Midrib	Center	Large Graveyard area 1
9	Taka Melor	Lateral vein	Center	Large Graveyard area 1
10	Taka Melor	Lateral vein	Apex	Large Graveyard area 1
11	Taka Melor	Lateral vein	Apex	Large Graveyard area 1
12	Taka Melor	Lateral vein	Center	Large Graveyard area 1
13	Taka Melor	Lateral vein	Center	
14	Taka Melor	Lateral vein	Center	
15	Taka Melor	Midrib	Apex	
16	Hutan Simpan Labis	Lateral vein	Center	
17	Hutan Simpan Labis	Lateral vein	Center	
18	Hutan Simpan Labis	Lateral vein	Center	
19	Hutan Simpan Labis	Midrib	Center	Small Graveyard Area 1
20	Hutan Simpan Labis	Midrib	Apex	Small Graveyard Area 1
21	Hutan Simpan Labis	Midrib	Apex	Small Graveyard Area 1
22	Hutan Simpan Labis	Lateral vein	Center	Small Graveyard Area 1
23	Sungai Bantang, Bekok	Lateral vein	Center	
24	Sungai Bantang, Bekok	Midrib	Apex	
25	Sungai Bantang, Bekok	Lateral vein	Center	
26	Sungai Bantang, Bekok	Lateral vein	Center	
27	Sungai Bantang, Bekok	Midrib	Base	
28	Sungai Bantang, Bekok	Midrib	Center	

Enhanced Knowledge in Sciences and Technology Vol. 4 No. 2 (2024) p. 635-648

29	Sungai Bantang, Bekok	Lateral vein	Center	Small Graveyard Area 2
30	Sungai Bantang, Bekok	Lateral vein	Center	Small Graveyard Area 2
31	Sungai Bantang, Bekok	Lateral vein	Base	Small Graveyard Area 2
32	Sungai Bantang, Bekok	Midrib	Apex	Small Graveyard Area 2
33	Sungai Bantang, Bekok	Midrib	Apex	Small Graveyard Area 3
34	Sungai Bantang, Bekok	Midrib	Apex	Small Graveyard Area 3
35	Sungai Bantang, Bekok	Midrib	Apex	Small Graveyard Area 3
36	Sungai Bantang, Bekok	Midrib	Apex	Small Graveyard Area 3
37	Sungai Bantang, Bekok	Midrib	Apex	Small Graveyard Area 4
38	Sungai Bantang, Bekok	Midrib	Center	Small Graveyard Area 4
39	Sungai Bantang, Bekok	Lateral vein	Center	Small Graveyard Area 4
40	Sungai Bantang, Bekok	Midrib	Apex	Small Graveyard Area 4
41	Sungai Bantang, Bekok	Lateral vein	Apex	Small Graveyard Area 4
42	Sungai Bantang, Bekok	Midrib	Apex	Large Graveyard area 2
43	Sungai Bantang, Bekok	Midrib	Apex	Large Graveyard area 2
44	Sungai Bantang, Bekok	Midrib	Apex	Large Graveyard area 2
45	Sungai Bantang, Bekok	Midrib	Apex	Large Graveyard area 2
46	Sungai Bantang, Bekok	Midrib	Apex	Large Graveyard area 2
47	Sungai Bantang, Bekok	Midrib	Apex	Large Graveyard area 2
48	Sungai Bantang, Bekok	Midrib	Apex	Large Graveyard area 2
49	Sungai Bantang, Bekok	Midrib	Center	Large Graveyard area 2
50	Sungai Bantang, Bekok	Lateral vein	Apex	Large Graveyard area 2
51	Sungai Bantang, Bekok	Midrib	Center	Large Graveyard area 2
52	Sungai Bantang, Bekok	Midrib	Apex	Large Graveyard area 2
53	Sungai Bantang, Bekok	Midrib	Center	Large Graveyard area 2
54	Sungai Bantang, Bekok	Midrib	Center	Large Graveyard area 2
55	Sungai Bantang, Bekok	Lateral vein	Center	Large Graveyard area 2
56	Sungai Bantang, Bekok	Midrib	Apex	Large Graveyard area 2
57	Sungai Bantang, Bekok	Midrib	Apex	Large Graveyard area 2
58	Sungai Bantang, Bekok	Midrib	Apex	Large Graveyard area 2
59	Sungai Bantang, Bekok	Midrib	Center	Large Graveyard area 2
60	Sungai Bantang, Bekok	Twig	Branch	Large Graveyard area 2
61	Sungai Bantang, Bekok	Midrib	Apex	Large Graveyard area 2
62	Sungai Bantang, Bekok	Midrib	Apex	Large Graveyard area 2
63	Sungai Bantang, Bekok	Midrib	Apex	Large Graveyard area 2
64	Sungai Bantang, Bekok	Lateral vein	Apex	Large Graveyard area 2
65	Sungai Bantang, Bekok	Lateral vein	Apex	Large Graveyard area 2
66	Sungai Bantang, Bekok	Midrib	Center	Large Graveyard area 2
67	Sungai Bantang, Bekok	Midrib	Center	Large Graveyard Area 3
68	Sungai Bantang, Bekok	Midrib	Apex	Large Graveyard Area 3
69	Sungai Bantang, Bekok	Lateral vein	Center	Large Graveyard Area 3
70	Sungai Bantang, Bekok	Lateral vein	Center	Large Graveyard Area 3
71	Sungai Bantang, Bekok	Lateral vein	Center	Large Graveyard Area 3
72	Sungai Bantang, Bekok	Midrib	Apex	Large Graveyard Area 3
73	Sungai Bantang, Bekok	Midrib	Apex	Large Graveyard Area 3
74	Sungai Bantang, Bekok	Lateral vein	Center	Large Graveyard Area 3
75	Sungai Bantang, Bekok	Midrib	Apex	Large Graveyard Area 3
76	Sungai Bantang, Bekok	Midrib	Apex	Large Graveyard Area 3
77	Sungai Bantang, Bekok	Midrib	Apex	Large Graveyard Area 3
78	Sungai Bantang, Bekok	Lateral vein	Center	Large Graveyard Area 3
79	Sungai Bantang, Bekok	Midrib	Center	Large Graveyard Area 3
80	Sungai Bantang, Bekok	Midrib	Center	Large Graveyard Area 3
81	Sungai Bantang, Bekok	Lateral vein	Center	
82	Sungai Bantang, Bekok	Lateral vein	Center	
83	Sungai Bantang, Bekok	Lateral vein	Center	
84	Sungai Bantang, Bekok	Lateral vein	Center	Large Graveyard Area 4
85	Sungai Bantang, Bekok	Midrib	Center	Large Graveyard Area 4

86	Sungai Bantang, Bekok	Lateral vein	Center	Large Graveyard Area 4
87	Sungai Bantang, Bekok	Lateral vein	Base	Large Graveyard Area 4
88	Sungai Bantang, Bekok	Lateral vein	Center	Large Graveyard Area 4
89	Sungai Bantang, Bekok	Lateral vein	Center	Large Graveyard Area 4
90	Sungai Bantang, Bekok	Lateral vein	Center	Large Graveyard Area 4
91	Sungai Bantang, Bekok	Lateral vein	Center	Large Graveyard Area 4
92	Sungai Bantang, Bekok	Lateral vein	Center	Large Graveyard Area 4

References

[1] Abdullahl, N., St, V., Yusoffl, M., & Desjardin, D. E. (2015).) Higher fungi of Northeast Langkawi. *Malaysian.Journal of Science* 24:95-102

[2] Andersen, S. B., Gerritsma, S., Yusah, K. M., Mayntz, D., Hywel-Jones, N. L., Billen, J., Boomsma, J. J., & Hughes, D. P. (2009). The life of a dead ant: the expression of an adaptive extended phenotype. American Naturalist, 174(3), 424–433. https://doi.org/10.1086/603640

[3] Anghel, D., Lascu, A., Epuran, C., Fratilescu, I., Ianasi, C., Birdeanu, M., & Fagadar-Cosma, E. (2020). Hybrid materials based on silica matrices impregnated with Pt-porphyrin or PtNPs destined for CO2 gas detection or for wastewaters color removal. *International Journal of Molecular Sciences*, 21(12), 1–19. https://doi.org/10.3390/ijms21124262

[4] Awg Abdul Rahman, A., & Mohamed, M. (2019). Checklist of Butterflies (Lepidoptera: Papilionoidea) of Sg. Bantang, Labis Forest Reserve, Johor. IOP Conference Series: Earth and Environmental Science, 269(1). https://doi.org/10.1088/1755-1315/269/1/012042

[5] Bencurova, E., Gupta, S. K., Sarukhanyan, E., & Dandekar, T. (2018). Identification of Antifungal Targets based on Computer Modeling. *Journal of Fungi* (Vol. 4, Issue 3). MDPI AG. https://doi.org/10.3390/jof4030081

[6] Blackwell, M. (2011). The fungi: 1, 2, 3 ... 5.1 Million Species? *American Journal of Botany*, 98(3), 426–438. https://doi.org/10.3732/ajb.1000298

[7] Butt, T. M., Coates, C. J., Dubovskiy, I. M., & Ratcliffe, N. A. (2016). Entomopathogenic Fungi: New Insights into Host-Pathogen Interactions. Advances in Genetics, 94, 307–364. https://doi.org/10.1016/bs.adgen.2016.01.006

[8] De Bekker, C., Quevillon, L. E., Smith, P. B., Fleming, K. R., Ghosh, D., Patterson, A. D., & Hughes, D. P. (2014). Species-specific ant brain manipulation by a specialized fungal parasite. BMC Evolutionary Biology, 14(1). https://doi.org/10.1186/s12862-014-0166-3

[9] Dong, C. H., & Yao, Y. J. (2011). On the reliability of fungal materials used in studies on *Ophiocordyceps Sinensis*. *Journal of Industrial Microbiology and Biotechnology*, 38(8), 1027–1035. https://doi.org/10.1007/s10295-010-0877-4

[10] Hebert, P. D. N., Cywinska, A., Ball, S. L., & DeWaard, J. R. (2003). Biological identifications through DNA barcodes. Proceedings of the Royal Society B: Biological Sciences, 270(1512), 313–321. https://doi.org/10.1098/rspb.2002.2218

[11] Hibbett, D. S., Binder, M., Bischoff, J. F., Blackwell, M., Cannon, P. F., Eriksson, O. E., Huhndorf, S., James, T., Kirk, P. M., Lücking, R., Thorsten Lumbsch, H., Lutzoni, F., Matheny, P. B., McLaughlin, D. J., Powell, M. J., Redhead, S., Schoch, C. L., Spatafora, J. W., Stalpers, J. A., … Zhang, N. (2007). A higher-level phylogenetic classification of the Fungi. Mycological Research, 111(5), 509–547. https://doi.org/10.1016/J.MYCRES.2007.03.004

[12] Hussin, Y. A., Azman, N. M., & Yusoff, M. K. (2017). Assessing local communities' attitudes and perceptions toward ecotourism activities in Endau Rompin National Park, Johor, Malaysia. *Journal of Sustainability Science and Management*, 12(1), 86–97.

[13] Kirk, M., Cannon, P., David, J., & Stalpers, J. (2002). Book Review Dictionary of the Fungi, ninth edition, by P. In Mycopathologia (Vol. 155). Oxford University Press.

[14] Luangsa-ard, J., Tasanathai, K., Thanakitpipattana, D., Khonsanit, A., & Stadler, M. (2018). Novel and interesting *Ophiocordyceps* sp. (Ophiocordycipitaceae, Hypocreales) with superficial perithecia from Thailand. Studies in Mycology, 89, 125–142. https://doi.org/10.1016/j.simyco.2018.02.001

[15] Lücking, R., Hodkinson, B. P., & Leavitt, S. D. (2017). The 2016 classification of lichenized fungi in the Ascomycota and Basidiomycota – Approaching one thousand genera. The Bryologist, 119(4), 361. https://doi.org/10.1639/0007-2745-119.4.361

[16] Mohd. Yusoff, A. F., Rahman, M. A., Abdul-Latiff, M. A., & Ramli, R. (2018). Mammalian diversity and abundance in Endau Rompin National Park, Johor, Malaysia (Vol. 29).

[17] Nilsson, R. H., Larsson, K. H., Taylor, A. F. S., Bengtsson-Palme, J., Jeppesen, T. S., Schigel, D., Kennedy, P., Picard, K., Glöckner, F. O., Tedersoo, L., Saar, I., Kõljalg, U., & Abarenkov, K. (2019). The UNITE database for molecular identification of fungi: Handling dark taxa and parallel taxonomic classifications. Nucleic Acids Research, 47(D1), D259–D264. https://doi.org/10.1093/nar/gky1022

[18] Nordin, N. H., Rahman, M. Z. A., & Johar, F. (2015). Mapping vegetation cover in Endau Rompin National Park using remote sensing and GIS techniques. *Journal of Environmental Science and Engineering* B, 4(9), 502–510.
[19] Samson, R. A., Visagie, C. M., Houbraken, J., Hong, S. B., Hubka, V., Klaassen, C. H. W., Perrone, G., Seifert, K. A., Susca, A., Tanney, J. B., Varga, J., Kocsubé, S., Szigeti, G., Yaguchi, T., & Frisvad, J. C. (2014). Phylogeny, identification and nomenclature of the genus Aspergillus. Studies in Mycology, 78(1), 141–173. https://doi.org/10.1016/j.simyco.2014.07.004
[20] Taberlet, P. (2007) Power and limitations of the chloroplast trnL(UAA) intron for plant DNA barcoding. Nucleic Acids Res.
[21] Tasanathai, K., Noisripoom, W., Chaitika, T., Khonsanit, A., Hasin, S., & Luangsa-Ard, J. (2019). Phylogenetic and morphological classification of *Ophiocordyceps* species on termites from Thailand. MycoKeys, 56, 101–129. https://doi.org/10.3897/mycokeys.56.37636
[22] Tedersoo, L., Sánchez-Ramírez, S., Kõljalg, U., Bahram, M., Döring, M., Schigel, D., May, T., Ryberg, M., & Abarenkov, K. (2018). High-level classification of the Fungi and a tool for evolutionary ecological analyses. Fungal Diversity, 90(1), 135–159. https://doi.org/10.1007/s13225-018-0401-0
[23] Yaakop, S., Shuib, A., Ismail, S., Ahmad, A., & Noor, I. A. M. (2016). Ecotourism development in Endau Rompin National Park, Johor, Malaysia: Perspectives and strategies for sustainable tourism. *Journal of Tourism, Hospitality, and Culinary Arts*. 8, 1–14.
[24] Zhou, X. W., Li, L. J., & Tian, E. W. (2014). Advances in research of the artificial cultivation of *Ophiocordyceps* sinensis in China. Critical Reviews in Biotechnology, 34(3), 233–243. https://doi.org/10.3109/07388551.2013.79124
[25] Felsenstein, J. 1985. Phylogenies and the comparative method. *The University of Chicago Press Journals* 125(1):1-15.
[26] Saitou, N. & Nei, M. 1987. The Neighbor-joining method: a new method for reconstructing phylogenetic tree. Molecular Biology and Evolution 4(4):406- 425.
[27] Kimura, M., 1980. *A simple method for estimating evolutionary rates of base substitutions through comparative studies of nucleotide sequences. Journal of Molecular Evolutionary* 16(2):111-120.
[28] Tang D, Zhao J, Lu Y, Wang Z, Sun T, Liu Z, Yu H (2023) Morphology, phylogeny and host specificity of two new *Ophiocordyceps* species belonging to the "zombie-ant fungi" clade (Ophiocordycipitaceae, Hypocreales). MycoKeys 99: 269-296. https://doi.org/10.3897/mycokeys.99.107565
[29] White TJ, Bruns T, Lee S, et al. (1990). Amplification and direct sequencing of fungal ribosomal RNA genes for phylogenetics. In: PCR Protocols: A Guide to Methods and Applications (Innis MA, Gelfand DH, Sninsky JJ, White TJ, eds). Academic Press, New York: 315–322.
[30] Vilgalys R, Sun BL (1994). Ancient and recent patterns of geographic speciation in the oyster mushroom Pleurotus revealed by phylogenetic analysis of ribosomal DNA sequences. Proceedings of National Academy of Sciences 91: 4599–4603.